Flow boundary conditions from nano- to micro-scales

Lydéric Bocquet

Université Lyon I Laboratoire de Physique de la Matière Condensée et des Nanostructures; CNRS,
UMR 5586, 43 Bvd. du 11 Nov. 1918, 69622 Villeurbanne Cedex, France

Jean-Louis Barrat

Université de Lyon; Univ. Lyon I, Laboratoire de Physique de la Matière Condensée et des Nanostructures; CNRS,
UMR 5586, 43 Bvd. du 11 Nov. 1918, 69622 Villeurbanne Cedex, France

(Dated: February 3, 2008)

The development of microfluidic devices has recently revived the interest in "old" problems associated with transport at, or across, interfaces. As the characteristic sizes are decreased, the use of pressure gradients to transport fluids becomes problematic, and new, interface driven, methods must be considered. This has lead to new investigations of flow near interfaces, and to the conception of interfaces engineered at various scales to reduce flow friction. In this review, we discuss the present theoretical understanding of flow past solid interfaces at different length scales. We also briefly discuss the corresponding phenomenon of heat transport, and the influence of surface slip on interface driven (e.g. electro-osmotic) flows.

I. INTRODUCTION

The nature of boundary conditions of fluid at solid surfaces has been revisited over the recent years. Beyond the fondamental understanding of the fluid-solid dynamics, the reason for such a strong interest lies in its potential applications in microfluidics. The driving of liquids in ever tiny channels raises a number of difficulties, one being the huge increase in hydrodynamic resistance when the channel size decreases. Releasing the no-slip boundary condition at the surfaces, and thereby allowing for boundary slippage, would allow to bypass this stringent conditions by decreasing wall friction. There is therefore a big hope to take benefit of slippage for microfluidic applications.

Many experiments have been performed on the subject, with sometimes contradicting results. We refer to the review of Lauga, Brenner and Stone for an exhaustive discussion of the experimental approaches to investigate slippage [1]. While experimental investigations focused first on slippage on bare (atomically smooth) surfaces, more recent works have turned towards structured surfaces, in particular superhydrophobic surfaces, characterized by patterns at the micro- or nano-scales.

In this review we concentrate on the theoretical understanding and expectations for the fluid-solid boundary condition. In particular, we will discuss the relevant theoretical framework for mechanisms that take place at different scales, and lead to slippage at solid-fluid interfaces.

II. FLOW PAST IDEAL INTERFACES/

From a conceptual standpoint, the simplest situation that can be considered is that of a semi infinite solid, bounded by an atomically smooth surface, in contact with a liquid that occupies the second half space. By atomically smooth, we mean for example a dense plane of a perfect crystalline lattice. The location of this lattice plane defines the xOy plane. The theoretical question becomes then simply to describe momentum transfer from the fluid to the solid (assumed here to be at rest) in terms of the velocity field existing in the fluid. Let us consider the case, where the fluid is undergoing a laminar, planar Couette flow in the x direction, e.g. driven by a second flat boundary far away in the z direction. In a stationary state, the stress component σ_{xz} is uniform, and the velocity profile of a Newtonian fluid reads, far away from the solid wall

$$v_x(z) = \dot{\gamma} z + v_s \qquad (1)$$

The shear stress is $\eta \dot{\gamma}$, where η is the shear viscosity of the bulk fluid and $\dot{\gamma}$ the shear rate. By definition, v_s is the slip velocity. To achieve a complete hydrodynamic description of the system, a constitutive equation involving the interface has to be introduced. Such a constitutive equation is generally described as a "boundary condition". Although we will also use this traditional vocabulary, we emphasize that it is somewhat misleading. In many cases, "boundary conditions" are seen as auxiliary mathematical constraints that allow to solve partial differential equations. In our mind, the status of the constitutive equation relative to the interface is in every respect comparable to the one of the bulk equations, e.g.

- it is a material property, involving the chemical nature of the two phases that create the ideal interface.

- it should be amenable to the same type of microscopic justifications and statistical mechanical treatments as bulk properties.

- it can be extracted unambiguously from transport measurements.

As for any constitutive equation, the writing of the interfacial constitutive equation involves a first step of
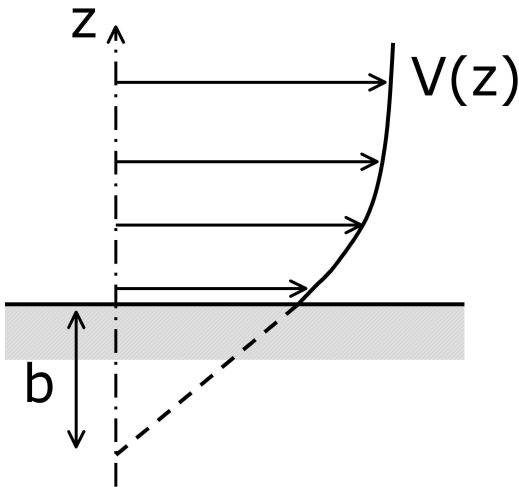
FIG. 1: Schematic representation of the definition of the slip length b

modeling based on considerations of symmetry and linearity. The simplest possible relation, consistent with the general description for newtonian fluids, assumes that the tangential stress exerted on the solid surface is proportional to the slip velocity, i.e.

$$\sigma_{xz} = \kappa v_s \qquad (2)$$

Combining (2) with the constitutive equation for the bulk Newtonian fluid, $\sigma_{xz} = \eta \partial_z v_x$, one arrives at the so called Navier boundary condition

$$v_s = \frac{\eta}{\kappa} \partial_z v_x = b \partial_z v_x \qquad (3)$$

which can be used as a boundary condition (in the mathematical sense) that complements the Navier-Stokes equation inside the fluid. This boundary condition is applied within one atomic distance of the first solid plane [2], where the stress (3) acts on the solid. By construction, the "hydrodynamic" flow that results from using this boundary condition will be identical to the actual, macroscopic flow far away from the boundaries. At the microscopic level, a thin interfacial region exists in which the flow may differ from the hydrodynamic calculation. We insist that this region, in which the velocity field can be obtained only from molecular scale studies, is not our main concern here. Studies at the molecular scales may result into velocity profiles that are not solution of the Stokes equation, or need to artificially introduce a position dependent viscosity.

The second equality in (3) introduces the *slip length* $b = \eta/\kappa$. The significance of this length is illustrated in figure 1, as the distance inside the solid to which the velocity profile has to be extrapolated to reach zero. The standard "no slip" boundary condition corresponds to $b = 0$, i.e. $\kappa \to \infty$. Conventionally a positive slip length is associated with a positive slip velocity, while

a (less common) negative length would indicate an apparent change in the sign of the velocity field near the solid. We emphasize that b is not an interfacial property in the usual sense, rather it is the ratio of a truly interfacial property, the friction κ, to a bulk property, the viscosity η. In particular, b is, in principle, completely unrelated to the width of the interfacial region alluded to above. All our knowledge of interfaces between solids and simple liquids indicates that -if critical phenomena are excluded- the width of the interfacial region is at most of a few atomic diameters. The slip length, on the other hand, can (theoretically) be made to diverge by going to the limit of a perfectly flat (in the mathematical sense) solid wall. Such a procedure, on the other hand, would not significantly alter the width of the interfacial region.

The determination of the interfacial constitutive relation, often described as "measurement of the slip length", has been the subject of numerous experimental [1, 3, 4, 5, 6, 7] and theoretical [2, 8, 9, 10, 11, 12, 13] investigations in the past 20 years . In spite of the experimental difficulties associated with the definition of "ideal" surfaces in experiments, the combination of increasingly accurate measurement methods and of insights from simulation and theory has produced a rather complete understanding of the "ideal" situation discussed here. The results can be summarized as follows.

(i) The *linear* relation (3) can be used to describe results for simple liquids, within the range of experimentally accessible shear rates [7]. Numerically, non linear behavior has been reported for shear rates of order $10^8 s^{-1}$ for simple liquids [14].

(ii) The friction coefficient κ, and hence the slip length b, depend strongly on the strength of the solid liquid interactions. Early measurements [3, 4] were performed on fluid/solid interfaces that correspond to a "wetting" situation, with a low contact angle. These measurements clearly reported a "no slip" boundary condition, with a slip length smaller than the molecular dimensions.

(iii) When the interaction between liquid and solid becomes weaker, so that the contact angle of the liquid on the substrates increases, larger values of b can be measured, typically in the range 10-50 nanometers.

(iv) Points (ii) and (iii) correspond to a general trend, but there is not a unique correlation between contact angle and friction. Other factors, such as the crystallinity of the solid, do influence the friction κ [8, 15].

These findings can be rationalized within the context of a linear response theory [2, 9] (see also [16]), which has been successfully compared to molecular simulations [9, 12]. A possible starting point is the Kubo like formula, which relates the interfacial transport coefficient for momentum (i.e. the friction κ) to the integral of the autocorrelation function of the momentum flux (i.e. the force exerted by the liquid on the solid):

$$\kappa = \frac{S}{k_B T} \int_0^\infty dt \langle f_x(t) f_x(0) \rangle \qquad (4)$$

where S is the surface area, and $f_x(t)$ is the tangential stress (force per unit area) exerted by the fluid on the solid at time t in the x direction[62]. Note that this formula can obviously be generalized to the case where κ would be anisotropic, represented by a 2×2 matrix, as would be the case for a surface of low symmetry. We will limit ourselves to the standard case of isotropic friction. Kubo formula such as (4) cannot in general be evaluated analytically. The correlation function can be computed in direct numerical simulations, or approximated using the standard methods of liquid state theory.

A simple approximation of the result of equation (4) was derived in [9], and allows one to quantify the main ingredients that enter the friction. The approximate expression reads

$$\kappa \simeq \frac{S_\parallel(q_0)}{D_\parallel k_B T} \int_0^\infty dz \rho(z) V_{FS}(z)^2 \qquad (5)$$

Here q_0 is the first wave-vector of the reciprocal lattice of the crystalline substrate; $S_\parallel(q_0)$ is the structure factor of the fluid evaluated for this wave-vector, in the interfacial region; $D_\parallel$ is a collective diffusion coefficient computed at the wave-vector q_0; $\rho(z)$ is the density profile of the fluid perpendicular to the interface, and $V_{FS}(z)$ is the interaction potential between a molecule in the fluid and the solid wall. The physical content of the various factors entering (5) is clear. The structure factor describes the response of the fluid to the fixed atomic corrugation of the solid wall. A large $S_\parallel(q_0)$ indicates "commensurability" of some sort between the liquid and the solid, which will increase momentum transfer. The diffusion constant sets, roughly, the time scale for the decay of stress-stress correlations.

Note that when κ is divided by η to obtain $1/b$, the product $D_\parallel \eta$ will be formed. For simple liquids, this ratio is typically equal to $k_B T$ divided by a molecular size σ, so that any explicit reference to the microscopic dynamics disappears from the resulting expression for the slip length.

$$b \simeq \frac{(k_B T)^2}{S_\parallel(q_0)\sigma \int_0^\infty dz \rho(z) V_{FS}(z)^2} \qquad (6)$$

It is therefore expected to be independent of the fluid viscosity for simple liquids.

The last important factor is the integral, which involves the wall fluid interaction and the density profile. It is through this integral, that the wetting properties of the fluid with respect to the solid enter the friction κ. As a crude approximation, let us assume that the density profile consists of a layer of density ρ_c (the "contact density") within a molecular thickness σ, followed by a bulk density ρ_B. We moreover assume van der Waals interactions with Hamaker constant A_H. Then the integral can be crudely approximated by $(A_H^2/\rho_B \sigma^2) \times (\rho_c/\rho_B)$.

Gathering the different ingredients that enter equation (5), it is easily seen that the only one that can display large variations is the "contact density", i.e. the average density of the liquid very close to the solid surface, typically within one molecular size, and, to some extent, the ratio $A_H/k_B T$. Both factors go into the same direction, namely large slip lengths are favored by a small liquid solid interaction. However, it is clear that, from a dimensional viewpoint, the integral $\int_0^\infty dz \rho(z) V_{FS}(z)^2$ will always remain a "molecular" quantity, so that the length scale that emerges from equation (6) is not expected to become very large unless very special state points are considered. In fact, our simulations show that the slip lengths that are achieved for simple Lennard-Jones models vary between a few molecular diameters and 50 to 60 molecular diameters, depending on the value of the interaction parameter that defines the solid liquid attraction (Hamaker constant). This is in very reasonable agreement, at a qualitative level, with the most recent experimental results [7].

The same framework may be applied to melts of short polymers. In this case, the substrate wave-vector q_0 is much larger than the inverse radius of gyration of the polymer, so that the collective diffusion is measured at the monomer scale : $D_\parallel$ is accordingly expected to be independent of the molecular weight N. This predicts that the ratio $D_\parallel \eta$ scales like η and increases with the polymer length, similar the predictions of de Gennes for longer chains [17]. This prediction and the validity of Eq. (5) has been exhaustively verified for short polymers (up to 16 monomers) using Molecular Dynamics simulations by Priezjev and Troian [12]. The experimental situation may be more complex since slippage will be strongly dependent on the polymer adsorption at the surface. Polymers also display strong nonlinear effects at moderate shear rates, which are not accounted for in our description, and have been extensively studied experimentally [18, 19] and theoretically [20].

Another interesting example of the use of equation (4) is the recent study of the influence of electrostatic effects on the solid-liquid friction in ionic solutions [21, 22]. A simple estimate of these effects based on Eq. (4) leads to an electrostatic friction contribution to the friction factor, varying as $\kappa' \propto \eta \Sigma^2 \ell_B$, with Σ the surface charge (in units of the elementary charge e), and $\ell_B = e^2/4\pi\epsilon k_B T$ the Bjerrum length (with ϵ the dielectric constant). Interestingly this contribution is independent of the Debye length.

While the theoretical and numerical descriptions converge unambiguously, a number of experimental reports have appeared over the years, that would appear to contradict either (i) or (ii) above, or both [5, 11, 23, 24]. In some cases, these discrepancies can be attributed to experimental artefacts associated with the measurement apparatus [7, 25]. However, another possible source of misunderstandings and errors lies in the structuration effects described below. The *intrinsic* constitutive boundary condition discussed in this section may be rather different from what is probed in flow experiments at larger length scales.

We conclude with a brief discussion of a view of the solid liquid interface which is sometimes proposed, in which the interfacial region is described as a "film" of thickness w_i, formed by some interfacial fluid (or vapor) of viscosity η_i. Standard "no slip" boundary conditions are applied at the film boundary. A straightforward calculation shows that, within this description, the friction κ that enters the constitutive equation for the interface is given by

$$\frac{1}{\kappa} = \left(\frac{1}{\eta_i} - \frac{1}{\eta}\right) w_i \tag{7}$$

and the equivalent slip length is

$$b = w_i \left(\frac{\eta}{\eta_i} - 1\right) \tag{8}$$

Such a description does not have a clear microscopic funding. In general, it is impossible to identify a "phase" with distinct properties at the interface. However, it gives a useful insight into the sensitivity of interfacial transport parameters to the structure of the interface. For example, assuming that the viscosity η_i is that of a vapor layer, it is easily shown that a slip length of 20nm corresponds to an interface thickness of just 0.25 nm (for water), hardly the size of a single molecule. Clearly this "layer" cannot correspond to a real phase, but is merely a very schematic representation of the depletion close to hydrophobic solid walls.

III. CLIMBING THE STRUCTURATION SCALE

A. Effective slippage on patterned surfaces

The situation of an atomically smooth surface, as described in the previous paragraph, involves basically two lengths scales : the microscopic scale, ℓ, characterizing the liquid-solid interface, typically of the order of the atomic size; and the macroscopic size $\mathcal{L}$, corresponding to the flow scale, e.g. the size of the channel in which the flow is conducted.

Intermediate scales may however be present, for example when the surface exhibits large scale structuration, associated with roughness or chemical patterns on a scale L. Assuming a scale separation between the different lengths, $\ell \ll L < \mathcal{L}$, the microscopic information associated with the liquid-solid dynamics may be integrated out and summarized in the local slip length on the patterned surface. In this case, the hydrodynamic quantities, velocity profile and pressure, do obey the Stokes equation, complemented by the local Navier condition with local slip lengths $\{b\}$ (of order ℓ) at the interface.

Once the solution of this set of equations has been calculated, it is possible to define an effective boundary condition, by integrating out the intermediate scale L. This introduces an effective slip length b_{eff}, which may be defined in terms of the friction force $\mathbf{F}_f$ on the solid interface and an averaged slip velocity $\langle V_s \rangle$, as :

$$\mathbf{F}_f = -\mathcal{A}\,\eta\,\frac{\langle V_s \rangle}{b_{\text{eff}}} \tag{9}$$

The averaged slip velocity $\langle V_s \rangle$ is computed in a given plane parallel to the interface and the effective slip length will thus depend on the specific choice for the location of this plane (e.g., top, bottom or mean of the roughness).

This definition of b_{eff} integrates out the modulation of the surface at the scale L. The effective slip length, b_{eff}, thus defines the effective boundary condition for the velocity profile v, *at scales larger than L* :

$$v_s = b_{\text{eff}} \partial_z v_x \tag{10}$$

The friction force on the surface can be obtained from the pressure P and viscous stress tensor $\overline{\overline{\sigma}}$ at the solid interface $\partial\Sigma$:

$$\mathbf{F}_f = \int_{\partial\Sigma} \left(-P\mathbb{I} + \overline{\overline{\sigma}}\right) \cdot d\mathbf{S} \tag{11}$$

with $\mathbb{I}$ the unit tensor. From the previous definition, the calculation of the effective slip length therefore reduces to the resolution of the initial (pure) hydrodynamic problem, involving the evaluation of the hydrodynamic velocity field and pressure fields. These fields are obtained from Stokes equation, complemented by the *local* boundary condition on the interface, with local slip lengths $\{b\}$.

As a first example of such a procedure we consider the simple case of flow past a wavy solid surface. For simplicity we consider a flow velocity perpendicular to the modulation of the surface, so that the situation is effectively two dimensional. The effective slip length is obtained in terms of the geometrical parameters of the interface, the period $\lambda = 2\pi/q$ and amplitude u ($\ll \lambda$) of the roughness : $b_{\text{eff}} = \frac{\lambda}{2\pi} f(qu)$. In the case where a perfect slip boundary condition applies locally on the surface, one obtains $f(qu) \propto (qu)^{-2}$ [26], while for a local no-slip boundary condition on the surface, $f(qu) \propto (qu)^2$ [27]. In both cases, the effective boundary condition applies at the averaged position of the surface. Though simple, these results provide some interesting insights into the nature of effective boundary condition :

- The result for the perfectly slipping interface shows that roughness inevitably decrease slippage. The friction originates accordingly in the viscous dissipation as the fluid flows past the roughness pattern. This result was first pointed out by Richardson [28], who showed that the no-slip boundary condition measured at the macroscopic scale follows from the roughness of surfaces. Recent MD simulations confirm this result [6, 29].

- On the other hand the result for a wavy surface with a local no-slip boundary condition suggests an effective slip on a wavy no-slip surface, while an

increased dissipation is expected on a modulated surface. This is a direct consequence of the choice for the position of the boundary plane, where the effective boundary condition applies : for the above results the averaged position has been chosen. For a boundary plane position at the bottom of the interface, the effective slip length is shifted by $-u$ and thus negative, in agreement with the increased dissipation on the modulated surface. This shows that the effective BC applies at some position between the bottom and top of the roughness.

• The above results applies for a single surface. If the flow is conducted in a channel with two confining surfaces separated by a distance H, the above expressions for the effective slip lengths are modified, and do depend on H ! (see eg [27]). Such a dependence is exhibited when the gap size compares with the roughness period $H \lesssim \lambda$. This points to the fact that effective boundary condition is *not* a characteristic of the liquid-solid interface solely, but may depend on the flow configuration when the surface modulation scale $L \equiv \lambda$ becomes comparable (or larger) than the flow scale $\mathcal{L} \equiv H$.

B.   Slippage on superhydrophobic surfaces

Another situation which has been the object of a strong interest over the recent years is that of superhydrophobic surfaces. These surfaces combine hydrophobicity at the molecular scale with roughness at intermediate scales, leading to the so-called "Lotus leaf effect" [30]. The roughness amplifies the natural non-wetting caracter of the surface, leading to very large contact angles - up to 175° for a liquid drop on the surface. We consider here the situation where the liquid surface remains at the top of the roughness (Cassie state). The liquid surface is in contact with the solid only through a small fraction ϕ_s of the surface, while the remaining is free-standing. At the hydrodynamic level, this composite surface leads to a spatially dependent boundary condition with a no-slip boundary condition on the real solid-liquid interface (with fraction ϕ_s), while the remaining surface is characterized by a perfect slip boundary condition ($b = \infty$) on the liquid-vapor interface.

Although the hydrophobicity of the surface at the molecular scale tends (according to the discussion of section II) to increase the slip length at small scale, the essential role of hydrophobicity is here a structural rather than dynamical one. The rough hydrophobic surface replaces part of the liquid solid interface with a stress free liquid vapour interface.

This problem has been first tackled theoretically by Philip [31] and more recently by Lauga and Stone [32] and Cottin-Bizonne *et al.* [33]. Several numerical approaches have also been proposed either at the molecular scale, using molecular dynamics [34], or at larger mesoscopic
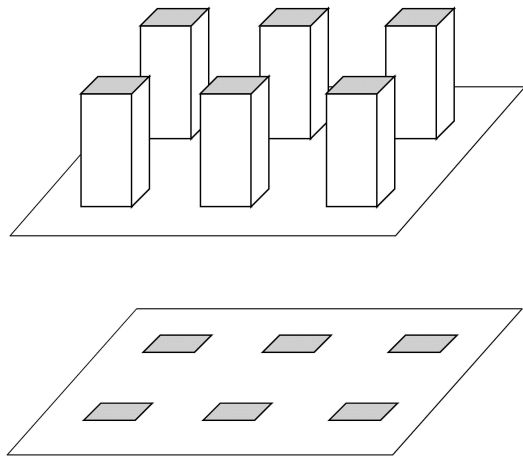

FIG. 2: Schematic representation of a surface patterned with nanoposts, and equivalent representation in terms of flow boundary conditions.

scales using finite element methods, Lattice Boltzmann or phase field models [35, 36, 37]. For a pattern composed of stripes, the expression for the effective slip length b_{eff} depends on the direction of the flow. For a flow parallel to the stripes, b_{eff} reads :

$$b_{\text{eff}} = \frac{L}{\pi} \log\left(\frac{1}{\cos[\frac{\pi}{2}(1 - \phi_s)]}\right) \qquad (12)$$

For a flow in the direction perpendicular to the flow, the result is given by the above expression divided by a factor 2. These expressions exhibit a weak (logarithmic) dependency on ϕ_s. In practice, the logarithmic term only varies in the interval $[0.4; 1.0]$ for ϕ_s between 0.1 and 5%, *i.e.* for feasible surfaces.

At a qualitative level, the theoretical results for the stripes can be summarized by stating that the effective slip length b_{eff} essentially saturates at the value fixed by the lateral scale of the roughness L, with an unfavorable prefactor ($1/(2\pi)$ in Eq. (12)). For example Eq. (12) shows that a slip length larger than the period of the pattern, $b_{\text{eff}} = L$, is obtained only when $\phi_s \leq 10^{-3}$. A large slippage is therefore difficult to obtain within the stripe geometry.

Another, more 'natural', geometry is that of a pattern of posts (see figure 2). In this case the hydrodynamic model consists in assuming a flat interface with a no-slip BC on the top of the posts, while the remaining of the surfaces obeys a shear-free BC.

No analytical resolution of Stokes equation with this set of boundary conditions has been performed up to now. However a simple 'scaling' argument accounts for the effective slip length in the limit of a small fraction ϕ_s of solid zones [38]. The friction force on the surface reduces to the force on the solid zones $F_f = \mathcal{A}\phi_s \eta \dot{\gamma}_s$, with $\dot{\gamma}_s$ the averaged shear rate on the solid patch. To estimate $\dot{\gamma}_s$, one may note that the velocity profile in the liquid is influenced by the solid zones only in a region of their size, a, in all directions : this behavior is due

to the Laplacian character of the Stokes equation obeyed by the fluid velocity. One therefore expects $\dot{\gamma}_s \sim U/a$, where U is the slip velocity of the fluid on the free slip zones. Therefore $F \simeq \mathcal{A}\phi_s \eta U/a$. Now the effective slip length is defined by $F_f = \mathcal{A}V/b_{\text{eff}}$, with $V \approx U$ the slip velocity. One therefore deduces, in the limit $\phi_s \to 0$,

$$b_{\text{eff}} \propto \frac{a}{\phi_s}. \qquad (13)$$

For a pattern made of individual posts, $\phi_s = (a/L)^2$, and $b_{\text{eff}} \sim L^2/a \sim L/\sqrt{\phi_s}$. A numerical resolution of the Stokes equation with a pattern of no-slip square dots confirms the validity of the heuristic argument above in the limit of small ϕ_s (basically $\phi_s < 40\%$) [38]. It moreover gives the prefactor of the predicted relationship, which is very close to $1/\pi$, so that [38] (in the limit $\phi_s \to 0$):

$$b_{\text{eff}} \simeq \frac{1}{\pi} \frac{L}{\sqrt{\phi_s}} \qquad (14)$$

This simple prediction would deserve an analytical justification, which has not been performed up to now.

We note that the above argument is independent of the geometry of the pattern - posts or stripes - and one should recover the expression in Eq. (12) for stripes. For solid zones made of stripes, we have $\phi_s = a/L$, so that $b_{\text{eff}} \sim L$: up to slowly varying logarithmic terms, this is in good agreement with the Philip-Lauga-Stone prediction, $b_{\text{eff}} \sim L/\log(1/\phi_s)$. As we emphasized above, in this geometry, the effective slip length is mainly fixed by the roughness period, L.

From the experimental point of view, several experimental studies have been conducted to measure slippage effects on superhydrophobic surfaces. Using pressure drop experiments, Rothstein and coworkers have reported slip lengths in the micron range on patterns of stripes [39, 40], with periodicity of the stripe in the tens of microns range (up to 150μm). Experiments are in good agreement with the prediction of hydrodynamic model of Philip [31]. More recently Choi et al. performed slip measurements on the same geometry but with nanoscale patterns [41], showing a slip length of a few hundred of nanometers, again in agreement with theoretical hydrodynamic predictions.

On surfaces made of a pattern of pillars and using rheological measurements, Choi and Kim [42] reported slip lengths in the tens of micron range on a surface made of nanoposts, $b_{\text{eff}} \simeq 20\mu$m for water. The expression for the slip length on dilute posts derived above, $b_{\text{eff}} \simeq \frac{1}{\pi}L/\sqrt{\phi_s}$, requires a very small solid fraction in their case to reach a 20μm slip length (with $L \sim 1\mu$m) : $\phi_s \sim 0.03\%$. The contact angle on such surfaces with ultra-low solid fractions is expected to be very close to $180\circ$: with this solid fraction a contact angle of $179°$ i sexpected, on the basis of the Cassie relationship [43], and assuming a contact angle of $\theta_0 = 110°$ on the solid posts. Contact angles $\sim 180°$ are indeed reported by Choi and Kim for their 'nanoturf' surface [42]. Note that the slip length is strongly dependent on the solid fraction in this regime : for example a slip length of 4.5μm is predicted for a solid fraction of $\phi_s = 0.5\%$, corresponding to a contact angle of $175°$. More recently, and using also rheological measurements, Truesdell et al. report huge slippage (in the millimeter range) for surfaces with a strip geometry [44], while $\phi_s \sim 50\%$ in their case. This result is at odds with theoretical expectations and would require further verifications. This points to the experimental difficulties to measure slippage effects inherent to rheological measurements, see Ref. [45]. Eventually, we mention the results of Joseph et al. who measured slip length on superhydrophobic carbon nanotube carpets using microparticle velocimetry (μ-PIV)measurements. Slip lengths in the micron range are found and measured to be proportional to the underlying pattern period L (with fixed surface fraction of solid $\phi_s \sim 0.15$ in their case) [46]. This results is in full agreement, both qualitative and quantitative, with theoretical predictions of Eq. (14).

As an overall conclusion, these results and predictions do show that very large slip lengths may be obtained only at the expense of important efforts to obtain nano-engineered surfaces with very small solid fraction. Typically, slip length larger than tens of microns are expected only with micro-patterned surfaces for which the measured contact angle is larger than $178°$. This is a very stringent condition.

C. Effective boundary condition on porous surfaces

In this context, it is interesting to point out the differences and similarities between our approach of ideal or structured interfaces and the approach used in the field of porous media. Effective slip boundary conditions at the interface between a bulk liquid and a porous media have been introduced empirically by Beavers and Joseph [47, 48, 49], and strongly resemble equation (2). They can be justified on the basis of matching a Brinkman description of the flow field in the porous media

$$\eta_{e}ff\nabla^2\mathbf{v} - \nabla P = \frac{\eta}{K}\mathbf{v} \qquad (15)$$

with the standard Stokes flow in the fluid. The resulting boundary condition is

$$\partial_z v_x(0) = \sqrt{\frac{\eta_{eff}/\eta}{K}}(v_x(0) - U) \qquad (16)$$

where K is the permeability of the porous medium, and $U = -K\nabla P$ is the drainage velocity deep inside the porous wall. This condition is often empirically modified to account for variations in the local permeability or viscosity near the interface [49]. From a conceptual viewpoint, this approach is different from the one described in section II, as it does not attribute physical properties to the interface. Rather, the usual hydrodynamic approach is used everywhere, with particular approximations relevant to porous media. The approach described in the

present section is somewhat closer in spirit, with the difference that it uses essentially exact results to describe the flow in the interfacial region.

IV. ANALOGY WITH THERMAL BOUNDARY CONDITIONS

An interesting analogy can be established between the flow of a fluid past a solid interface [50], and the flow of heat (or energy) transport across an interface. Let us consider two media (1 and 2) separated by an ideal planar interface perpendicular to the z axis, and a steady heat flux $\mathbf{J} = J\mathbf{e}_z$ perpendicular to the interface. Each medium is assumed to be described by Fourier's law, with conductivity κ_i. The temperature profile in medium i is linear

$$T_i(z) = \frac{J}{\kappa_i}z + T_i(0) \qquad (17)$$

The temperature jump at the interface, $T_1(0) - T_2(0)$, is the exact analog of the slip velocity. Again, note that $T_i(0)$ can be defined unambiguously as extrapolations of the bulk temperature field in the interface region, without any reference to a local temperature at the interface. A constitutive equation for the interfacial region is written in analogy with equation (2)

$$T_i(0) - T_2(0) = \frac{1}{R_K}\mathbf{J}\dot{\mathbf{n}}_{12} \qquad (18)$$

Equation (18) defines the Kapitsa resistance R_K (also known as thermal boundary resistance), as the transport coefficient describing the thermal effect of the interface. In order to complete the analogy with the slip length, a "Kapitsa length" ℓ_K can be defined using a suitable thermal conductivity, e.g. κ_1. $\ell_K = R_K\kappa_1$ is then the the thickness of material 1 which is thermally equivalent to the interface.

This transport coefficient has been extensively studied in the context of semiconductor physics, where the resistance can be interpreted in terms of phonon scattering at the interface [51]. It is also well known in the field of superfluid liquid helium [51] (where Kapitsa originally introduced the notion), where the very large conductivity of Helium II makes the effect particularly important. A Kubo formula similar to (4) can be formulated and reads [50, 52]

$$\frac{1}{R_K} = \frac{S}{k_B T}\int_0^\infty dt\langle q(t)q(0)\rangle \qquad (19)$$

where $q(t)$ is the heat flux (per unit area) across the interface at time t, and S is the interfacial area.

For simple fluid/solid interfaces, the effect of the Kapitsa resistance has attracted much less attention. In the recent years a number of numerical and experimental studies have appeared, motivated in particular by the interest in thermal properties of "nanofluids" (colloidal solution of oxide or metallic particles). The general trend from simulation results [50, 53] is that the Kapitsa length will depend on the interfacial or wetting properties in a way that is comparable to the slip length. A weaker affinity between the solid and the liquid, will result in higher resistances. Other ingredients, that are irrelevant for the slip length, include the difference in acoustic impedance between the liquid ans the solid [54]. Experimental studies involve transient absorption or transient reflectivity experiments [55, 56]. Typical values found for $G = 1/R_K$ are in the range $50 - 300\text{GW.m}^{-2}.\text{K}^{-1}$, with the smallest values obtained for hydrophobic interfaces in contact with water [53, 56]. This corresponds to a Kapitsa length (using the heat conductivity of water) of order 12nm, indeed comparable to the slip length at similar interfaces. If an attempt to model such a resistance through an "equivalent vapor layer" is made, a thickness of the order of one molecular size is found. This shows again that such transport coefficients are intrinsically interfacial properties, that cannot be assigned to the existence of a different "phase" at the interface.

We are not aware of any theoretical or experimental studies of heat transport across structured interfaces similar to those studied above for the slip properties. Obviously, strong effects, involving thermally driven dewetting, could be expected in the case of structured hydrophobic surfaces.

V. THE EXPECTED BENEFITS OF SLIPPAGE

A. permeability and hydrodynamic dispersion

One of the reason for the recent interest in slippage is that it may facilitate flows in micrometric chanel, *e.g.* for microfluidic purposes. A simple calculation shows that for a pressure drop flow in a slit with thickness h and slip length b on the surfaces, the mean velocity is increased by a factor $1 + 6b/h$ as compared to the no-slip surfaces [63]. Slippage thus increases the permeability of channels and porous materials. A second interesting property of slip flows is the reduction of hydrodynamic dispersion of a probe transported in the channel using a pressure drop flow. This dispersion originates in the vanishing velocity at the surface, while it is maximum in the middle of the channel. For slipping surfaces, the velocity does not vanish at the surface, thereby reducing the difference between the maximum and minimum velocities. A criterium for dispersion may be defined as $\Delta v = (v_{max} - v_{min})/v_{max}$, which for a slipping channel equals $\Delta v = (1 + 4b/h)^{-1}$.

For both phenomena, the efficiency of slippage is determined by the ratio b/h. This shows that micrometric slip lengths have to be reached for the slippage effects to be relevant for microfluidic purposes. As discussed above, this requires a specific engineering of the surfaces since slip lengths on bare surfaces are well below the micron ($b \sim 20$nm for water on hydrophobic surfaces). For
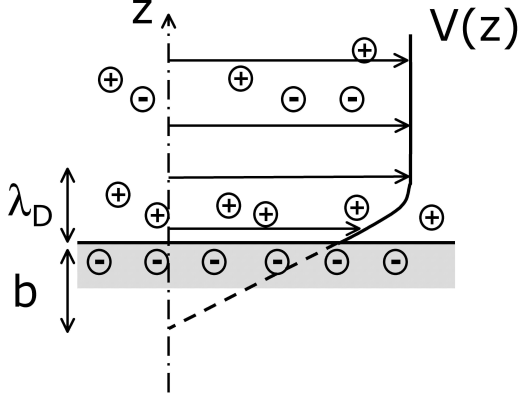
FIG. 3: Schematic representation of electro-osmotic flow past a slippery surface.

example, for a channel with size $H \sim 10\mu$m and a slip length $b \sim 20$nm, the increase of permeability is of order of one percent ! For a slip length $b \sim 2\mu$m as measured *e.g.* in [46], this permeability is more than twice its value for no-slip surfaces.

B. Interfacial transport phenomena

The above discussion relies on the fact that the flow is driven on the scale of the channel h. However alternative methods do generate flows within the interfacial structure at the solid-liquid interface. Electro-osmosis, *i.e.* flow generation by an electric field, is one such example which is commonly used in microfluidics. As discussed in references [57, 58, 59] these interfacially driven transport phenomena are considerably amplified by surface slippage, *even for nanometric slip length*. The reason for this amplification is that slip length b now compares with the thickness of the interfacial structure λ, and one expects a amplification ratio for the transport of order b/λ. For typical conditions, this ratio is larger than one even for nanometric slip lengths and slippage strongly increase the efficiency of interfacial transport phenomena.

Let us precise the underlying mechanisms on the example of electro-osmosis. Under the application of an electric field E, the solvent acquires a plug flow like velocity profile, with a velocity v_{EO} proportional to E and given by the Smoluchowski formula :

$$v_{EO} = -\frac{\epsilon \zeta}{\eta} E \qquad (20)$$

with ϵ the dielectric permittivity of the solvent, η its viscosity; ζ is the Zeta potential of the surface, which is traditionally assumed to match the electrostatic potential at the position where the velocity profile vanishes (the shear-plane position) [60].

Electro-osmosis originates within the Debye layer at the interface [60]. The Debye layer quantifies the width of the interfacial regions at a charged surface and results

from the competition between the attraction of ions at the charged surface and entropic effects. Its typical size λ_D depends on the salt concentration in the liquid, and is of the order of a few nanometers : $\lambda_D \sim 3$nm for a concentration of salt of 10^{-2} molar. The interfacial Debye layer is electrically charged, while the remaining bulk solvent is electrically neutral. Therefore, when applying an electric field, the electric driving force is located within the Debye layer only. The driving force per unit surface acting on the liquid thus writes $f_e = \sigma E$ with σ the charge of the Debye layer, which is exactly opposite to the surface charge $\sigma \simeq \epsilon V_0/\lambda_D$, for weak surface potentials V_0. This leads to $f_e \simeq -\epsilon \frac{V_0}{\lambda_D} E$. Now the electro-osmotic velocity results from the balance between this electric driving force in the Debye layer and the viscous stress at the surface. For a no-slip boundary condition, the latter is $f_\eta \sim \eta v_{EO}/\lambda_D$, since the velocity varies on a scale given by the Debye length. If slippage is exhibited at the surface, the velocity varies on the size $\lambda_D + b$ and the viscous stress becomes accordingly $f_\eta = \eta v_{EO}/(\lambda_D + b)$, lower than for the no-slip BC. Gathering these results we get

$$\eta \frac{v_{EO}}{\lambda_D + b} \sim -\epsilon \frac{V_0}{\lambda_D} E \qquad (21)$$

This simple argument leads to the Smoluchowski formula, Eq. (20), and provides an expression of the zeta potential in the form

$$\zeta = V_0 \left(1 + \frac{b}{\lambda_D} \right) \qquad (22)$$

This expression can be obtained using more rigourous description, see [21, 57, 59]. Molecular dynamics simulations of charge transport confirm fully this relationship [21, 57]. They show, furthermore, that for a non-slipping surface V_0 can be identified with the potential at the plane of shear $V_0 = V(z_s)$, with z_s of the order of one liquid layer. As expected a strong amplification of charge transport is therefore demonstrated on slipping surfaces.

This behaviour can be generalized to all interfacial transport phenomena. As practical examples, one may cite diffusio-osmosis and thermo-osmosis. These two phenomena correspond to the induction of a flow by the gradient of a solute concentration for the former and by a gradient of temperature for the latter [61]. The flow velocity for these phenomena is found to be proportional to the applied gradient of the observable O under consideration (electric potential, concentration, temperature) :

$$v_s = -\frac{1}{\eta} \Gamma L.[1 + b/L].\frac{dO}{dx} \qquad (23)$$

Γ and L defined in terms of the (equilibrium) interfacial stress anisotropy, $\Sigma_{eq}(x,y) = \sigma_n - \sigma_t$: $\Gamma = \int_0^\infty dy.\frac{\partial \Sigma_{eq}}{\partial O}(y)$, and $L = \Gamma^{-1}\int_0^\infty dy.y.\frac{\partial \Sigma_{eq}}{\partial O}(y)$. These quantities are length scales of the order of the range of interaction of the solute with the solid surface [58]

The origin of the phenomena thus lies in the thin interface layer of size L where the solute interacts specifically with the surface. For the diffusio-osmosis phenomena, the driving force is an osmotic pressure gradient within the interface layer. For thermo-osmosis, this is surface energy gradient induced by the temperature dependence of the stress anisotropy.

For all these phenomena, slippage again amplifies the transport phenomena with a ratio b/L. Slippage, even nanometric, is therefore relevant to amplify interfacial transport in microfluidic systems.

VI. PERSPECTIVES

In this short review, we have tried to establish a clear picture of our present understanding of slippage at different scales. At the molecular scale, we consider surfaces as ideal and introduce an "intrinsic" constitutive relation for the interface. The corresponding slip length depends strongly on the nature of intermolecular interactions (hydrophobicity effect), but stays within "molecular" orders of magnitude, a few ten nanometers at most.

A different picture is obtained by considering surfaces structured on an intermediate scale. To describe such situations, we adopt a mesoscopic view of the interface, in which the molecular details are hidden in a local, position dependent slip length. Such a view can be validated through molecular simulations. Hydrophobicity effects are essential to reduce the contact area between solid and liquid, so that a significant reduction of the solid-liquid friction is obtained. When this reduction is achieved, much larger slip lengths can be observed. The slip length is essentially determined by the scale of the surface pattern and the surface area of the "dewetted" part, on which a perfect slip boundary condition applies at the local level.

This description at two different levels is necessary to describe the full complexity of surfaces that can now be engineered at a submicrometer scale, with a combination of local hydrophobic properties and of a complex geometric pattern. For patterns whose typical scale is much larger than the intrinsic slip length, the separation of lengths scales allows a complete decoupling between the molecular and the hydrodynamic descriptions. Molecular simulations indicate that the same type of approach is possible, even when the length scale of the pattern and the intrinsic slip length are similar.

From this complete theoretical description, it is clear that the control of actual flow properties through surface engineering necessitates a control of the surface state at each different scale. When such a control is achieved, the flow of simple liquids appear to be relatively well understood, both experimentally and theoretically. More complex situations, such as the amplification of interface driven flows by molecular slippage described in section V B, have not been studied experimentally in detail yet, but are promising for the design of microfluidic devices.

In section IV we discussed the analogy between "temperature slip" and "velocity slip". Experiments and simulations have already shown that this analogy can be made quantitative, at least when ideal surfaces are concerned. The role of nano-structuration of the surfaces for thermal transport has not been explored up to now. Nonlinear effects may be expected for strong heat fluxes, while cross effects between heat and momentum transport are expected to be negligible, based on symmetry arguments.

Finally, it could be interesting, at least from a formal point of view, to extend the above discussion of heat and momentum transport across an interface to diffusive mass transport. The standard description assumes a local partition equilibrium at the interface, or equivalently a continuity of the chemical potential. Following the approach outlined here, it would seem more consistent to introduce a discontinuity in chemical potential proportional to the diffusive flux across the interface. The magnitude of this discontinuity has not, to our knowledge, be explored at the molecular scale.

[1] E. Lauga, M. P. Brenner, and H. A. Stone, in *Handbook of Experimental Fluid Dynamics*, edited by C. T. J. Foss and A. Yarin (Springer, 2005), chap. 15, to appear, `cond-mat/0501557`.

[2] L. Bocquet and J.-L. Barrat, Phys. Rev. E **49**, 3079 (1994).

[3] D. Y. C. Chan and R. G. Horn, J. Chem. Phys. **83**, 5311 (1985).

[4] J.-M. Georges, S. Millot, J.-L. Loubet, and A. Tonck, J. Chem. Phys. **98**, 7345 (1993).

[5] R. Pit, H. Hervet, and L. Léger, Phys. Rev. Lett. **85**, 980 (2000).

[6] C. Cottin-Bizonne, C. Barentin, E. Charlaix, L. Bocquet, and J.-L. Barrat, Eur. Phys. J. E **15**, 427 (2004).

[7] C. Cottin-Bizonne, B. Cross, A. Steinberger, and E. Charlaix, Phys. Rev. Lett. **94**, 056102 (2005).

[8] P. A. Thompson and M. O. Robbins, Phys. Rev. A **41**, 6830 (1990).

[9] J.-L. Barrat and L. Bocquet, Faraday Discuss. **112**, 119 (1999).

[10] M. Cieplak, J. Koplik, and J. R. Banavar, Phys. Rev. Lett. **86**, 803 (2001).

[11] Y. Zhu and S. Granick, Phys. Rev. Lett. **87**, 096105 (2001).

[12] N. V. Priezjev and S. M. Troian, Phys. Rev. Lett. **92**, 018302 (2004).

[13] A. Jabbarzadeh, P. Harrowell, and R. I. Tanner, J. Chem. Phys. **125** (2006).

[14] P. A. Thompson and S. M. Troian, Nature **389**, 360 (1997).

[15] P. A. Thompson, G. S. Grest, and M. O. Robbins, Phys. Rev. Lett. **68**, 3448 (1992).

[16] E. D. Smith, M. O. Robbins, and M. Cieplak, Phys. Rev. B **54**, 8252 (1996).

[17] P.-G. de Gennes, Comptes rendus de l'Acadmie des Sciences **288**, 219 (1979).

[18] L. Leger, H. Hervet, G. Massey, and et al., Journal Of Physics-condensed Matter **9**, 7719 (1997).

[19] R. Fetzer, M. Rauscher, A. Munch, and et al., Europhysics Letters **75**, 638 (2006).

[20] F. Brochardwyart, P. G. Degennes, H. Hervert, and et al., Langmuir **10**, 1566 (1994).

[21] L. Joly, C. Ybert, L. Bocquet, and E. Trizac, Houille Blanche-revue Internationale De L Eau pp. 53–58 (2006).

[22] L. Joly, C. Ybert, and L. Bocquet, J. Chem. Phys **in press** (2006).

[23] C. Neto, D. R. Evans, E. Bonaccurso, H. J. Butt, and V. S. J. Craig, Reports On Progress In Phys. **68**, 2859 (2005).

[24] E. Bonaccurso, H.-J. Butt, and V. S. J. Craig, Phys. Rev. Lett. **90**, 144501 (2003).

[25] O. I. Vinogradova and G. E. Yakubov, Langmuir **19**, 1227 (2003).

[26] P.-G. de Gennes, Langmuir **18**, 3413 (2002).

[27] A. D. Stroock, S. K. Dertinger, G. M. Whitesides, and et al., Analytical Chemistry **74**, 5306 (2002).

[28] S. Richardson, J. Fluid Mech. **59**, 707 (1973).

[29] C. Cottin-Bizonne, J.-L. Barrat, L. Bocquet, and E. Charlaix, Nature Mat. **2**, 237 (2003).

[30] D. Quere, Reports On Progress In Phys. **68**, 2495 (2005).

[31] J. R. Philip, Z. Angew. Math. Phys. **23**, 960 (1972).

[32] E. Lauga and H. A. Stone, J. Fluid Mech. **489**, 55 (2003).

[33] C. Cottin-Bizonne, C. Barentin, E. Charlaix, L. Bocquet, and J. L. Barrat, European Phys. J. E **15**, 427 (2004).

[34] C. Cottin-Bizonne, S. Jurine, J. Baudry, J. Crassous, F. Restagno, and E. Charlaix, Houille Blanche-revue Internationale De L Eau pp. 116–119 (2003).

[35] N. Priezjev, A. Darhuber, and S. Troian, Phys. Rev. Lett. **71**, 041608 (2005).

[36] R. Benzi, L. Biferale, M. Sbragaglia, S. Succi, and F. Toschi, Mathematics Computers In Simulation **72**, 84 (2006).

[37] J. Harting, C. Kunert, and H. J. Herrmann, Europhysics Lett. **75**, 328 (2006).

[38] C. Ybert, C. Barentin, C. Cottin-Bizonne, and L. Bocquet, submitted to Physics of Fluids (2007).

[39] J. Ou, B. Perot, and J. P. Rothstein, Phys. Fluids **16**, 4635 (2004).

[40] J. Ou and J. P. Rothstein, Phys. Fluids **17** (2005).

[41] C. H. Choi, U. Ulmanella, J. Kim, C. M. Ho, and C. J. Kim, Phys. Fluids **18** (2006).

[42] C. H. Choi and C. J. Kim, Phys. Rev. Lett. **96** (2006).

[43] M. Callies and D. Quere, Soft Matter **1**, 55 (2005).

[44] R. Truesdell, A. Mammoli, P. Vorobieff, and et al., Physical Review Letters **97**, 044504 (2006).

[45] L. Bocquet, P. Tabeling, and S. Manneville, Physical Review Letters **97**, 109601 (2006).

[46] P. Joseph, C. Cottin-Bizonne, C. Y. J.-M. Benoît, C. Journet, P. Tabeling, and L. Bocquet, Phys. Rev. Lett. **97**, 156104 (2006).

[47] D. D. Joseph, Journal Of Applied Mechanics **33**, 753 (1966).

[48] G. S. Beavers, Journal Of Fluid Mechanics **30**, 197 (1967).

[49] B. Goyeau, D. Lhuillier, D. Gobin, and et al., International Journal Of Heat And Mass Transfer **46**, 4071 (2003).

[50] J. L. Barrat and F. Chiaruttini, Molecular Physics **101**, 1605 (2003).

[51] E. T. Swartz and R. O. Pohl, Reviews Of Modern Physics **61**, 605 (1989).

[52] L. Puech, G. Bonfait, and B. Castaing, Journal Of Low Temperature Physics **62**, 315 (1986).

[53] H. A. Patel, S. Garde, and P. Keblinski, Nano Letters **5**, 2225 (2005).

[54] M. Vladkov and J. L. Barrat, Nano Letters **6**, 1224 (2006).

[55] O. M. Wilson, X. Y. Hu, D. G. Cahill, and et al., Physical Review B **66**, 224301 (2002).

[56] Z. B. Ge, D. G. Cahill, and P. V. Braun, Physical Review Letters **96**, 186101 (2006).

[57] L. Joly, C. Ybert, E. Trizac, and L. Bocquet, Phys. Rev. Lett. **93** (2004).

[58] A. Ajdari and L. Bocquet, Phys. Rev. Lett. **96** (2006).

[59] H. Stone, A. Stroock, and A. Ajdari, Ann. Rev. Flu. Mech. **36**, 381 (2004).

[60] R. J. Hunter, *Foundations of colloid science* (Oxford Univ. Press, Oxford, 2001), 2nd ed.

[61] J. L. Anderson, Annual Review Of Fluid Mechanics **21**, 61 (1989).

[62] A matrix generalization of 4 is easily obtained for anisotropic surfaces.

[63] A factor $1 + 8b/h$ is found for a cylindrical channel